Electronic correlations in graphite and carbon nanotubes from Auger spectroscopy

E. Perfetto,[1] M. Cini,[2,3] S. Ugenti,[2,3] P. Castrucci,[1,2] M. Scarselli,[1,2] M. De Crescenzi,[1,2] F. Rosei,[4] and M. A. El Khakani[4]

[1]*Unità CNISM, Università di Roma Tor Vergata, Via della Ricerca Scientifica 1, I-00133 Rome, Italy*
[2]*Dipartimento di Fisica, Università di Roma Tor Vergata, Via della Ricerca Scientifica 1, I-00133 Rome, Italy*
[3]*Istituto Nazionale di Fisica Nucleare—Laboratori Nazionali di Frascati, Via E. Fermi 40, 00044 Frascati, Italy*
[4]*Institut National de la Recherche Scientifique, INRS-Énergie, Matériaux et Télécommunications, Varennes, Quebec, Canada J3X 1S2*

We have determined the screened on-site Coulomb repulsion in graphite and single wall carbon nanotubes by measuring their Auger spectra and performing a theoretical analysis based on an extended Cini-Sawatzky approach [Solid State Commun. **24**, 681 (1977); Phys. Rev. Lett. **39**, 504 (1977)], where only one fit parameter is employed. The experimental line shape is very well reproduced by the theory, and this allows us to determine the value of the screened on-site repulsion between $2p$ states, which is found to be 2.1 eV in graphite and 4.6 eV in nanotubes. The latter is robust by varying the nanotube radius from 1 to 2 nm.

Carbon nanostructures continue to be an intense field of both fundamental and applied research because of the recent discoveries of several of their unusual physical properties. Among these, we can recall (i) the observation of the anomalous integer quantum Hall effect in planar graphene,[1,2] (ii) the measurement of superconductivity at 11.5 K in Ca intercalated graphite,[3] and (iii) intrinsic superconductivity in multiwall[5] and ultrasmall[4] carbon nanotubes at temperatures of 12 and 15 K, respectively. In the light of these unprecedented properties and related new physics, the study and the quantitative estimate of electronic correlations in these carbon nanostructures are of fundamental importance. In fact, in one-dimensional conductors, like metallic nanotubes, the electronic interactions have a dramatic impact on their electronic properties, giving rise to the so-called Luttinger liquid behavior. This manifests in the power-law dependence of observables such as the tunneling density of states (DOS), of which suppression at low energies has been observed in conductance measurements.[6,7] More importantly, the accurate estimate of the screened Coulomb repulsion is a challenging problem that should be dealt within any theoretical study aiming at addressing the question of superconductivity.

Auger electron spectroscopy is a powerful experimental tool which permits the characterization of the effective interaction between electrons in solids. In particular, the Auger line shape is proportional to the two-particle interacting DOS as a consequence of the creation of two valence holes on the same lattice site caused by the x-ray photoemission of a deep core electron. Several attempts have been made to interpret the Auger spectra of amorphous graphite[8] and highly oriented pyrolitic graphite (HOPG),[9] but a satisfactory description is still to come. Moreover, only a few experimental data on single wall carbon nanotube (SWCNT) Auger line shapes are available.[9] Furthermore, no theoretical effort introducing Coulomb repulsion in SWCNTs has been attempted so far.

In this Brief Report, we present a comparative study of the Auger spectra of HOPG and SWCNTs. Through a different theoretical analysis of the Auger experimental data, we provide an accurate estimate of the on-site screened repulsion in both carbon structures. The access to this quantity is key in realistic local density approximation +U calculations and in any low-energy interacting theory of the honeycomb lattice where only π Dirac-like electrons are considered.

SWNCTs were synthesized by ablating a CoNi-doped graphite target, using a pulsed Nd:YAG laser in the superposed double pulse configuration.[10] Raman spectroscopy indicated that the tube is single walled, characterized by a low degree of defects and with diameters of 1.2–1.3 nm.[10] This is consistent with transmission electron microscopy (TEM) observations that, though showing tubes aggregated in bundles of various dimensions and twisting, allowed us to measure a tube diameter of 1.2±0.1 nm through a statistical analysis.[11] Moreover, electron energy loss spectroscopy performed, by using the TEM apparatus, directly on SWCNTs bundles at the Co and Ni $L_{2,3}$ edges did not detect any traces of these catalysts.[12] A droplet of the synthesis product was diluted in isopropyl alcohol and dispersed on a metallic surface. A freshly cleaved HOPG sample was used for measuring the core-valence-valence (KVV) Auger features. The Auger spectra were acquired using an Al $K\alpha$ (1486.6 eV) x-ray source with a resolution of about 1 eV. The obtained experimental spectra are shown in Fig. 1 after subtraction of secondary electron background.

The Auger line shape of solids can be calculated by using the so-called two-step approach, in which the photoemission and the Auger decay are considered as independent events. In the absence of significant electronic correlations, the computation of KVV Auger spectrum reduces to the self-convolution of the one-particle valence DOS. If moderate or strong (compared to the bandwidth) on-site repulsion is present, the line shape can be calculated by means of the Cini-Sawatzky[13,14] approach.

Following Ref. 13, the Auger current J reads

$$J = \sum_{\alpha_1, \alpha_2, \alpha_3, \alpha_4, \sigma} A_{\alpha_1, \alpha_2, \alpha_3, \alpha_4, \sigma} D_{\alpha_1, \alpha_2, \alpha_3, \alpha_4, \sigma}(\omega), \qquad (1)$$

where α_i denote all the single-particle valence orbitals available in the solid, A is the so-called Auger matrix element given by
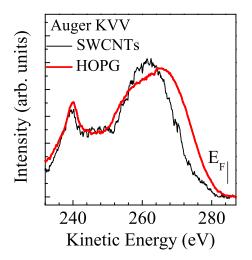
FIG. 1. (Color online) Experimental KVV Auger spectra of HOPG graphite (bold red/gray curve) and SWCNTs with average diameter of 1.3 nm (black curve).

$$A_{\alpha_1,\alpha_2,\alpha_3,\alpha_4,\sigma} = \sum_k \langle v|d_{\alpha_1\uparrow}d_{\alpha_2\sigma} \left| \frac{e^2}{r} \right| d^\dagger_{c\sigma_c}d^\dagger_{k\sigma_k}|v\rangle$$

$$\times \langle v|d_{c\sigma_c}d_{k\sigma_k} \left| \frac{e^2}{r} \right| d^\dagger_{\alpha_3\uparrow}d^\dagger_{\alpha_4\sigma}|v\rangle, \qquad (2)$$

with k,c and σ_k, σ_c denoting the Auger electron and core orbitals, and spin, respectively. D is the two-particle interacting DOS

$$D_{\alpha_1,\alpha_2,\alpha_3,\alpha_4,\sigma}(\omega) = \langle v|d_{\alpha_1\uparrow}d_{\alpha_2\sigma}|\delta(\omega-H)|d^\dagger_{\alpha_3\uparrow}d^\dagger_{\alpha_4\sigma}|v\rangle, \quad (3)$$

where H is the interacting Hamiltonian of the solid. Here, we denote by $|v\rangle$ the hole-vacuum and by $d_i^{(\dagger)}$ the annihilation (creation) operator of a hole in spin-orbital i. D is obtained as usual from the anti-Hermitian part of the two-particle Green's function $G_{\alpha_1,\alpha_2,\alpha_3,\alpha_4,\sigma}(\omega)$, which obeys the matrix Dyson[16] equation

$$G_\sigma = G_\sigma^{(0)}[1 + U_\sigma G_\sigma^{(0)}]^{-1}, \qquad (4)$$

where $G^{(0)}$ is the noninteracting two-hole Green's function and U is the matrix of screened on-site repulsion for valence states. The screened interaction differs from the bare atomic one, defined as

$$U^b_{\alpha_1,\alpha_2,\alpha_3,\alpha_4,\sigma} = \langle v|d_{\alpha_1\uparrow}d_{\alpha_2\sigma} \left| \frac{e^2}{r} \right| d^\dagger_{\alpha_3\uparrow}d^\dagger_{\alpha_4\sigma}|v\rangle. \qquad (5)$$

The evaluation of U starting from the atomic value U^b is generally a delicate task. In the following, we discuss the phenomenological approach we have adopted to determine this quantity. The Cini-Sawatzky approach works quite well in closed (or almost closed) band systems like zinc and copper, where the ladder approximation leading to Eq. (4) provides an exact result. However, if the Fermi level crosses the middle of the conducting band, the computation of the Auger current becomes a remarkably challenging many-body problem, which usually cannot be solved by evaluating Green's functions.[15]

In the light of this, the theoretical study of Auger spectra of HOPG and SWCNTs is, indeed, far from straightforward because the σ and π bands are half filled. However, in these systems, some special features (which are discussed hereafter) allow the use of closed-band theory, with slight but crucial modifications.

First, we observe that the DOS is largely suppressed in the proximity of the Fermi level, so that screening is not very efficient. This implies a static renormalization of the bare interaction U^b, which must be used in the theory. Second, we recall that the bonding portion of the $\sigma_{s,p}$ bands is separated by several eV from the antibonding part located above the Fermi level. As long as such a separation is larger than the effective interaction, one can treat the band as if it was closed, thus justifying the approach reported by Cini,[13] where no structural modification is needed for the interacting Green's function in Eq. (4). However, the situation is different for the π band, where the bonding and antibonding portions are separated by a very small region with a small DOS. Here, Cini's approach cannot be used without appropriate modifications. In this case, the contribution to the Auger spectrum originating from π and mixed π-σ holes would be strongly influenced by open-band effects. It is also expected that such a region should reveal the principal differences between the spectra of HOPG and SWCNTs. In fact, screening and excitonic effects[17] and Luttinger liquid properties in SWCNTs are expected to lead to a quite different behavior of electrons in proximity of the Fermi level due to the different dimensionality. This conjecture seems to be confirmed by the experimental data. Indeed, the π and mixed π-σ portions of the spectrum (i.e., $\omega \gtrsim 250$ eV) show clear differences between HOPG and SWCNTs, while in the σ_s region (i.e., $\omega \lesssim 250$ eV), the two spectra are quite similar. In particular, for 250 eV $\lesssim \omega \lesssim 280$ eV, the line shape of SWCNTs is narrower, with vanishing and much weaker intensity in proximity of the Fermi level, as compared to the one for graphite. This fits well with a scenario where the screening properties of π electrons are less efficient in SWCNTs.

Within the closed-band theory, the Auger spectrum is obtained by taking the Auger matrix elements and the on-site interactions from atomic calculations which neglect solid state effects. On this basis, one introduces the static screening operated by the closed-band system simply by rescaling all the $F^{(0)}(i,j)$ Slater integrals that enter the bare U^b, such that $F^{(0)}(i,j) \rightarrow F^{(0)}(i,j) - W$. W can be taken as the unique free fitting parameter of the theory. Alternatively, W can be also estimated within the random phase approximation or *ab initio* methods.[18] The only ingredient which accounts for the Auger holes being in the solid is the noninteracting one-particle DOS $\rho^{(0)}(\omega)$. Its self-convolution $D^{(0)}(\omega) = \int d\varepsilon \rho^{(0)}(\varepsilon)\rho^{(0)}(\omega-\varepsilon)$ and the corresponding Hilbert transform build the noninteracting G^0 entering Eq. (4).

Cini's approach should, in principle, be completed by introducing the effect of off-site interaction. Experiments on Au (Ref. 19) showed that there is a shift of 1.2 eV between the profile predicted by the above theory and experiment. The shift is 2.4 eV in the case of Ag.[20] This was explained in terms of the off-site interaction. In the two-hole resonance, there is an important amplitude where the holes sit on neighboring sites and, including the nearest-neighbor interaction
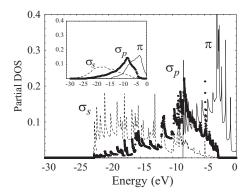
FIG. 2. One-particle partial DOS of (10,10) SWCNT (diameter close to 1.3 nm) obtained by the tight binding method of Ref. 22. The inset shows the same quantity for graphite, taken from Ref. 8. The Fermi level corresponds to zero energy and the antibonding part is not displayed.

into the theory, yields an almost rigid shift close to the experimental one.[21]

In the following, we will phenomenologically consider the open-band effects by introducing orbital-dependent *form factors* $f_{\alpha_1,\alpha_2,\alpha_3,\alpha_4}$. This must be introduced to correct all the quantities measuring *local* properties expressed by $\langle v|d_{\alpha_1}d_{\alpha_2}|O|d_{\alpha_3}^\dagger d_{\alpha_4}^\dagger|v\rangle$, where O is a local observable. Therefore, the effective on-site repulsions $U_{\alpha_1,\alpha_2,\alpha_3,\alpha_4,\sigma}$ (where F^0 has been already rescaled by W) and the matrix elements $A_{\alpha_1,\alpha_2,\alpha_3,\alpha_4,\sigma}$ will be corrected by a common multiplying factor $f_{\alpha_1,\alpha_2,\alpha_3,\alpha_4}$. In our case, the α_i states are σ_s, σ_x, σ_y, and π. The form factor f takes into account that the $2s$ states of carbon behave as if they were atomic, while the $2p$ ones are delocalized in the lattice. The latter can use only $1/2$ of the total σ_p and π states to form occupied localized states because the p bands are half filled. Therefore, we have three independent f factors corresponding to having (i) four σ_s orbitals, (ii) two σ_s and two $\sigma_{x,y}, \pi$ orbitals, and (iii) four $\sigma_{x,y}$, π orbitals in the quartet $\{\alpha_1,\alpha_2,\alpha_3,\alpha_4\}$. According to the above discussion, the three independent form factors are estimated to be $f_{ssss} \approx 1$, $f_{sspp} \approx 1/2$, and $f_{pppp} \approx 1/4$. We will show that this choice works quite well in the case of HOPG, while we need $f_{pppp} \approx 1/2$ to reproduce the Auger spectrum of nanotubes. Indeed, in nanotubes, the geometry constrains the holes and this could be the reason for a larger f_{pppp} than in graphite. It is worthwhile to note that the analysis of Ref. 21 does not apply to p holes and, in fact, no shift is seen in this case (the pairs presumably extend further than a nearest-neighbor distance). A shift could be present in the KL_1L_1 case, but we cannot distinguish since there is a single peak there.

We proceed by evaluating the noninteracting one-particle DOS $\rho^{(0)}$ for each kind of valence state. In the case of HOPG, we use the DOS from Ref. 8, which is taken from experiments. For SWCNTs, we performed a tight binding calculation[22] including both $2s$ and $2p$ orbitals, but neglecting overlap integrals for simplicity. The result for a typical (10,10) armchair nanotube with diameter close to 1.3 nm is shown in Fig. 2 together with the DOS of HOPG. For the Auger matrix elements, we used the (spin-independent) val-
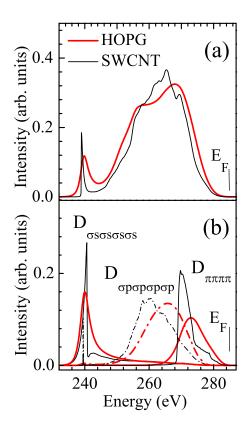

FIG. 3. (Color online) (a) Theoretical line shape [computed from Eq. (1)] of KVV Auger spectrum for HOPG (bold red/gray) and for SWCNTs (black) curve. (b) Diagonal contributions of the interacting DOS for HOPG (bold red/gray) and for SWCNTs (black), where the two valence holes have the same symmetry. The $D_{\sigma_p\sigma_p\sigma_p\sigma_p}$ contribution is understood as the sum $D_{\sigma_x\sigma_x\sigma_x\sigma_x} + D_{\sigma_y\sigma_y\sigma_y\sigma_y}$. The x axis displays kinetic energy, obtained by shifting the position of the Fermi level in Fig. 2 by 284.6 eV, which is the binding energy of $1s$ core hole.

ues $A_{ssss}=0.8$, $A_{sspp}=0.5$, and $A_{pppp}=1.0$, which are obtained by atomic calculations[8] and, hence, apply to both graphite and carbon nanotubes. The bare (atomic) on-site Coulomb repulsions are obtained by appropriate combinations of the Slater integrals $F^{(0,2)}(i,j)$ and $G^{(1)}(i,j)$ (Ref. 23) found in the literature.[24] The independent bare interactions are (in eV) $U^b_{ssss\downarrow}=15.5$, $U^b_{sxsx\downarrow}=15.0$, $U^b_{sxxs\downarrow}=1.5$, $U^b_{\pi\pi\pi\pi\downarrow}(\equiv U^b_{pppp})$ $=14.6$, $U^b_{xx\pi\pi\downarrow}=-0.1$, $U^b_{x\pi x\pi\downarrow}=13.9$, $U^b_{x\pi\pi x\downarrow}=0.8$, $U^b_{ssxx\downarrow}$ $=11.9$, and $U^b_{sxsx\uparrow}=U^b_{x\pi x\pi\uparrow}=13.1$. As discussed above, these values must be corrected by solid state effects. This is done by subtracting the screening constant W from the $F^{(0)}(i,j)$ Slater integrals and multiplying the resulting U and A matrix elements by the f factors (W being the only fitting parameter of our approach).

The theoretical spectra of HOPG and SWNCTs were computed by solving a 16×16 matrix problem for $\sigma=\downarrow$ and a 6×6 problem for $\sigma=\uparrow$, as shown in Eq. (4).[16] The final result is plotted in Fig. 3(a), where the best fit yielded the respective values $W_{HOPG}=6.0$ eV and $W_{SWCNT}=5.5$ eV for HOPG and SWCNTs. The agreement between theory and experiment is quite good, and is particularly satisfactory for graphite.

These values permit the determination of the most relevant parameter of our model, which is the screened on-site repulsion between the $2p$ states. Thus, the best fit for W yields $U_{pppp}=2.1$ eV for HOPG and $U_{pppp}=4.6$ eV for SWCNTs. This result gives rise to the lack of features close to the Fermi level for SWCNTs, making the Auger spectrum more symmetric and narrower than that of HOPG. This is understood by looking at Fig. 3(b), which shows the diagonal contributions of the interacting DOS according to Eq. (3), where the valence holes were taken in the same state. The off-diagonal contributions are not shown for the sake of clarity, but are essential to reproduce the experimental spectra.

Concerning the line shapes, the most striking feature is the narrow structure at 240 eV, which also appears as a shoulder in the spectrum reported by Houston *et al.*[8] This peak was assigned to a plasmon replica of the main structure at 265 eV, produced by a plasmon with an energy $\omega_p=27$ eV. Conversely, we interpret the narrow structure as a quasi-two-hole resonance produced by two σ_s Auger holes. This is consistent with the predicted values of the screened on-site repulsion between σ_s holes, which are $U_{ssss}=9.5$ and 10.0 eV for HOPG and SWCNTs, respectively. The noninteracting $D_{ssss}^{(0)}$ has a maximum at $\varepsilon_{ss}=252$ eV (graphite) and 251 eV (nanotube) and, therefore, a narrow structure around $\varepsilon_{ss}-U_{ssss}\approx241$ eV in the interacting D_{ssss} is correctly expected. Since the σ_s bandwidth is ~20 eV, a full splitoff two-hole resonance cannot happen, but a strongly distorted

bandlike behavior occurs (see Fig. 1b of Ref. 13). It is worth noting that the Auger spectrum from a sample consisting of SWCNTs with average diameter of 2 nm does not show significant changes with respect to that reported in Fig. 1. Moreover, by performing a similar theoretical analysis on a (20,20) SWCNT, no substantial changes can be found for the values of the correlation interaction. This means that the values we obtain for the correlation in SWCNTs have a very small dependence on the nanotube diameter.

In conclusion, the line shape of the Auger spectra for HOPG and SWCNTs has been interpreted in terms of a modified Cini-Sawatzky approach using a single fitting parameter. The U_{pppp} Coulomb repulsion results doubled, passing from HOPG to SWCNTs. This explains the sizable shift of the Auger feature at high kinetic energy measured for SWNTs, as compared to HOPG. Finally, we point out that the increase of the U_{pppp} value is consistent with the theoretical prediction[25] of the enhancement of the superconductive critical temperature observed recently in carbon nanotubes.

[1] K. S. Novoselov, A. K. Geim, S. V. Morozov, D. Jiang, M. I. Katsnelson, I. V. Grigorieva, S. V. Dubonos, and A. A. Firsov, Nature (London) **438**, 197 (2005).

[2] Y. Zhang, Y. W. Tan, H. L. Stormer, and P. Kim, Nature (London) **438**, 201 (2005).

[3] N. Emery, C. Hérold, M. d'Astuto, V. Garcia, Ch. Bellin, J. F. Marêché, P. Lagrange, and G. Loupias, Phys. Rev. Lett. **95**, 087003 (2005).

[4] Z. K. Tang, L. Zhang, N. Wang, X. X. Zhang, G. H. Wen, G. D. Li, J. N. Wang, C. T. Chan, and P. Sheng, Science **292**, 2462 (2001).

[5] I. Takesue, J. Haruyama, N. Kobayashi, S. Chiashi, S. Maruyama, T. Sugai, and H. Shinohara, Phys. Rev. Lett. **96**, 057001 (2006).

[6] Z. Yao, H. W. Ch. Postma, L. Balents, and C. Dekker, Nature (London) **402**, 273 (1999).

[7] M. Bockrath, D. H. Cobden, J. Lu, A. G. Rinzler, R. E. Smalley, L. Balents, and P. L. McEuen, Nature (London) **397**, 598 (1999).

[8] J. E. Houston, J. W. Rogers, Jr., R. R. Rye, F. L. Hutson, and D. E. Ramaker, Phys. Rev. B **34**, 1215 (1986).

[9] A. P. Dementjev, K. I. Maslakov, and A. V. Naumkin, Appl. Surf. Sci. **245**, 128 (2005).

[10] N. Braidy, M. A. El Khakani, and G. A. Botton, Carbon **40**, 2835 (2002).

[11] P. Castrucci, M. De Crescenzi, M. Scarselli, M. Diociaiuti, P. Chistolini, M. A. El Khakani, and F. Rosei, Appl. Phys. Lett. **87**, 103106 (2005).

[12] P. Castrucci, F. Tombolini, M. Scarselli, S. Bini, M. De Crescenzi, M. Diociaiuti, S. Casciardi, M. A. El Khakani, and F. Rosei, Phys. Rev. B **75**, 035420 (2007).

[13] M. Cini, Solid State Commun. **24**, 681 (1977).

[14] G. A. Sawatzky, Phys. Rev. Lett. **39**, 504 (1977).

[15] O. Gunnarsson and K. Schönhammer, Phys. Rev. B **22**, 3710 (1980).

[16] M. Cini, Phys. Rev. B **17**, 2788 (1978).

[17] J. E. Houston, D. E. Ramaker, J. W. Rogers, Jr., R. R. Rye, and F. L. Hutson, Phys. Rev. Lett. **56**, 1302 (1986).

[18] M. Cococcioni and S. de Gironcoli, Phys. Rev. B **71**, 035105 (2005).

[19] C. Verdozzi, M. Cini, J. A. Evans, R. J. Cole, A. D. Laine, P. S. Fowles, L. Duo, and P. Weightman, Europhys. Lett. **16**, 743 (1991).

[20] R. J. Cole, C. Verdozzi, M. Cini, and P. Weightman, Phys. Rev. B **49**, 13329 (1994).

[21] C. Verdozzi and M. Cini, Phys. Rev. B **51**, 7412 (1995).

[22] R. Saito, M. Fujita, G. Dresselhaus, and M. S. Dresselhaus, Phys. Rev. B **46**, 1804 (1992).

[23] See, for instance, M. Weissbluth, *Atoms and Molecules* (Academic, San Diego, 1978).

[24] J. B. Mann, *Atomic Structure Calculations* (National Technical Information Service, Springfield, VA, 1967).

[25] S. Bellucci, M. Cini, P. Onorato, and E. Perfetto, Phys. Rev. B **75**, 014523 (2007).